

THE OFFICIAL MAGAZINE OF THE OCEANOGRAPHY SOCIETY

# Oceanography

CITATION

Shcherbina, A.Y., E.A. D'Asaro, S.C. Riser, and W.S. Kessler. 2015. Variability and interleaving of upper-ocean water masses surrounding the North Atlantic salinity maximum. *Oceanography* 28(1):106–113, <http://dx.doi.org/10.5670/oceanog.2015.12>.

DOI

<http://dx.doi.org/10.5670/oceanog.2015.12>

COPYRIGHT

This article has been published in *Oceanography*, Volume 28, Number 1, a quarterly journal of The Oceanography Society. Copyright 2015 by The Oceanography Society. All rights reserved.

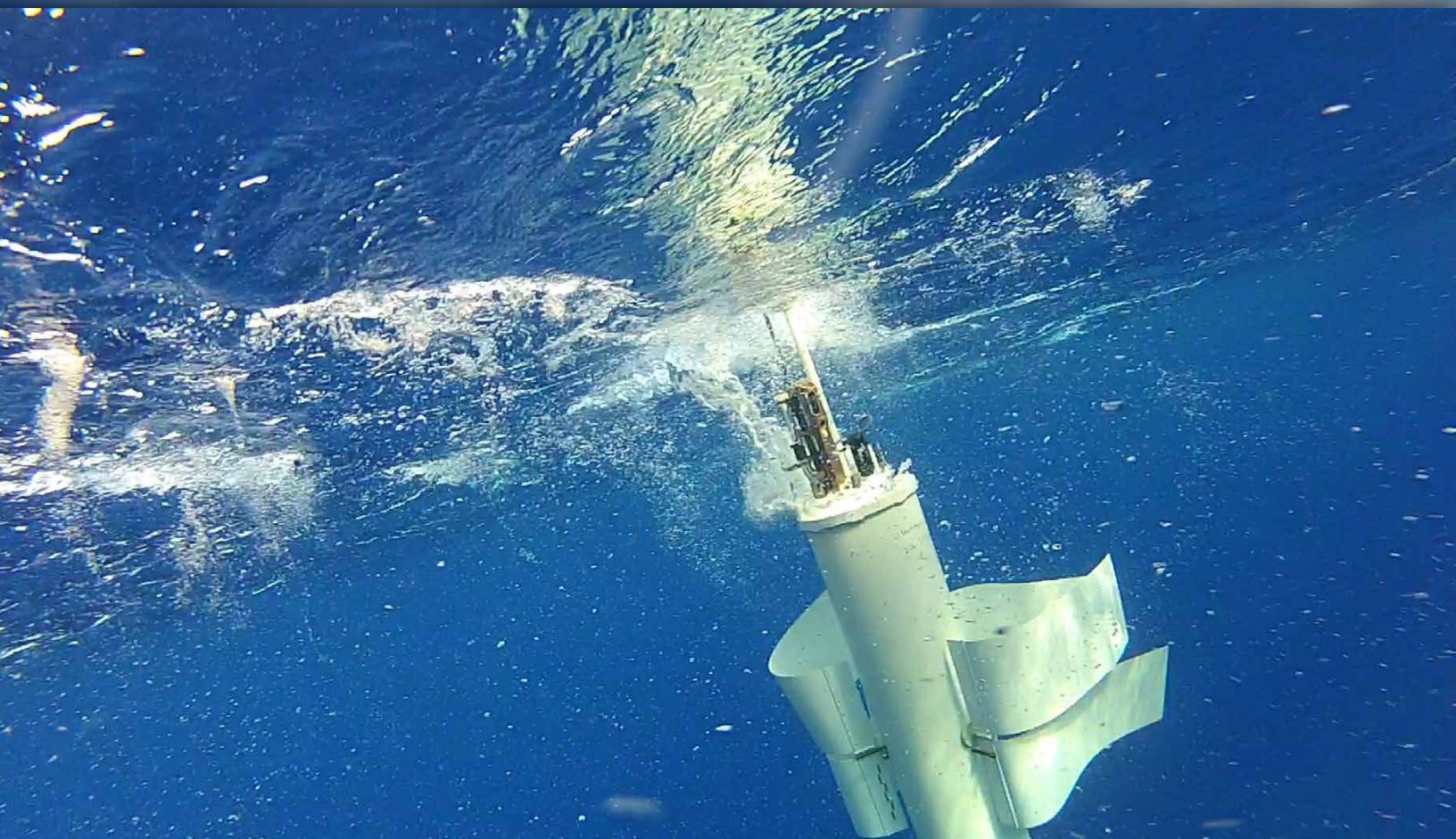
USAGE

Permission is granted to copy this article for use in teaching and research.

Republication, systematic reproduction, or collective redistribution of any portion of this article by photocopy machine, reposting, or other means is permitted only with the approval of The Oceanography Society. Send all correspondence to: [info@tos.org](mailto:info@tos.org) or The Oceanography Society, PO Box 1931, Rockville, MD 20849-1931, USA.

# Variability and Interleaving of Upper-Ocean Water Masses Surrounding the North Atlantic Salinity Maximum

By Andrey Y. Shcherbina, Eric A. D'Asaro,  
Stephen C. Riser, and William S. Kessler



**ABSTRACT.** The North Atlantic subtropical salinity maximum harbors the saltiest surface waters of the open world ocean. Subduction of these waters gives rise to Subtropical Underwater, spreading the high-salinity signature over the entire basin. The Salinity Processes in the Upper-ocean Regional Study (SPURS) is aimed at understanding the physics controlling the thermohaline structure in the salinity maximum region. A combination of moored and autonomous float observations is used here to describe the vertical water mass interleaving in the area. Seasonal intensification of interleaving in late spring and the abundance of small-scale thermohaline intrusions point to an important role for submesoscale processes in the initial subduction and subsequent evolution of Subtropical Underwater.

## INTRODUCTION

The highest sea surface salinities (SSS) in the world ocean are found in the interiors of subtropical gyres, owing to the excess of evaporation over precipitation and convergent surface currents in these regions. Of these high-salinity patches, the one in the North Atlantic reaches the highest open-ocean salinities, in excess of  $37 \text{ g kg}^{-1}$  (Talley, 2002; Gordon et al., 2015, in this issue). Not coincidentally, the subtropical North Atlantic is also the site of the strongest wind-driven (Ekman) convergence and downwelling, reaching  $50 \text{ m yr}^{-1}$  (Williams, 2001). Once subducted into the upper pycnocline, the high-salinity

water forms a distinct maximum in vertical profiles of salinity (Figure 1), referred to as Subtropical Underwater (STUW; O'Connor et al., 2005).

Subduction of North Atlantic high-salinity waters creates a “river of salt” that spreads its influence over the entire basin (Qu et al., 2013; Schmitt and Blair, 2015, in this issue). A part of the subducted water enters the subtropical cell, a shallow thermohaline overturn that connects with the equatorial current system (McCreary and Lu, 1994). Due to relatively high subduction rates and short residence times, subtropical cell overturns may play an important role in

controlling decadal climate variability of tropical regions (Nonaka et al., 2002). For the same reasons, STUW may also be a sensitive indicator for changes in global climate, as suggested by the observed systematic increase in North Atlantic STUW salinity between the 1960s and the 1990s (Curry et al., 2003).

Previous observational and modeling studies of North Atlantic STUW (O'Connor et al., 2005; Qu et al., 2013) focused on the mean climatological properties of this water mass, as well as the mechanisms and rates of its bulk formation and dispersal. Here, we focus on the origins of this water mass as it emerges from the North Atlantic SSS maximum region.

## SPURS OBSERVATIONS

In 2012–2013, the National Aeronautics and Space Administration (NASA) supported an intensive field observation campaign in the North Atlantic salinity maximum region—Salinity Processes in the Upper-ocean Regional Study (SPURS-1; Lindstrom et al., 2015, in this issue). An

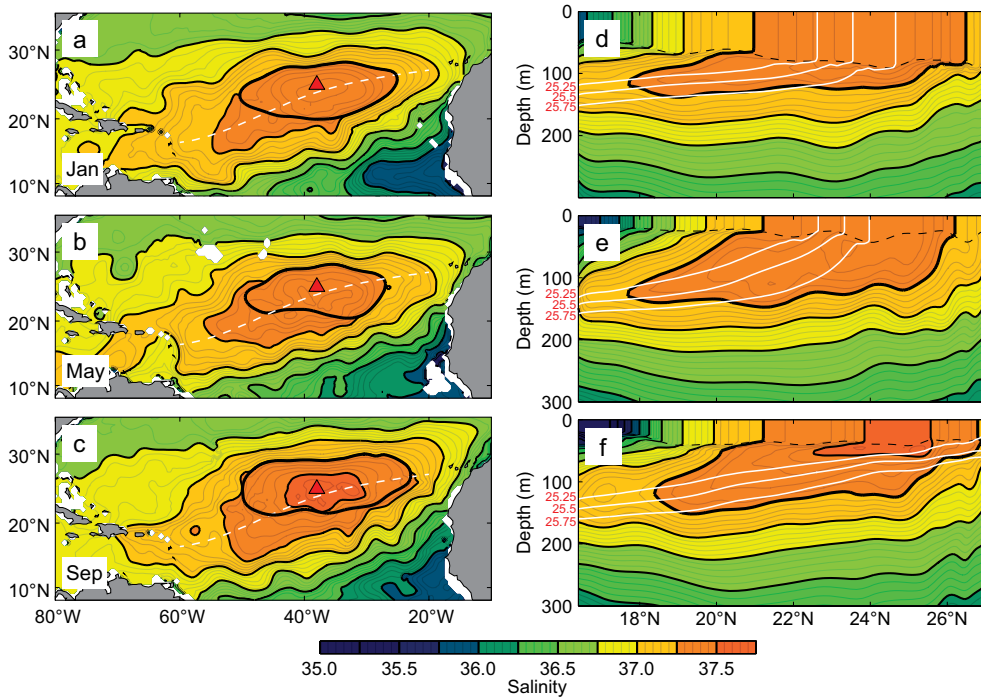


**FIGURE 1.** The Salinity Processes in the Upper-ocean Regional Study (SPURS) targeted Subtropical Underwater (STUW), a high-salinity water mass in the tropical North Atlantic. (a–c) Seasonal evolution of the vertically maximum climatological salinity based on Monthly Isopycnal/Mixed-layer Ocean Climatology (MIMOC; Schmidtko et al., 2013). The approximate axis of the maximum is indicated with a white dashed line. The surface expression of the 37.25 isohaline is marked by a thicker contour that roughly outlines the surface salinity maximum. Red triangles mark the location of the SPURS moorings. (d–f) Vertical salinity cross section along the salinity maximum axis (marked in a–c with white dashed lines). Several isopycnals in the  $25.25\text{--}25.75 \text{ kg m}^{-3}$  range are shown in white, with the potential density values indicated on the left. Black dashed lines mark the mixed-layer depth.

array of three moorings was deployed at approximately 24°40'N, 38°W (the “SPURS site,” marked with triangles in Figures 1 and 2) in the vicinity of the climatological surface salinity maximum. The heavily instrumented “central” mooring served as the focal point of the study (Farrar et al., 2015, in this issue). The “northern” and “eastern” moorings were National Oceanic and Atmospheric Administration (NOAA) Platform and Instrumentation for Continuous Observations (PICO) buoy systems equipped with wave-powered conductivity-temperature-depth (CTD) profilers (“Prawlers”). The wave energy drove the Prawlers up and down the mooring line to produce continuous profiles of temperature and salinity from about 15 m to 500 m every two to three hours.

The broad-scale SPURS-1 observations were conducted with an array of 16 APEX profiling floats deployed in a 200 km × 200 km square surrounding the moorings (see Riser et al., 2015, in this issue, for further details on the SPURS APEX float deployment). The SPURS APEX floats, which have the same components and capabilities as those used in the Argo program, supplemented the global profiling float array and ensured broad spatial coverage and continuity with historic measurements. These floats

had a typical parking depth of 1 km and profiled from 2 km to near-surface every 10 days. Several of the floats also operated in an alternative “fast-cycling” mode, profiling the upper 200 m at two-hour intervals for two to three weeks each.

Additionally, two Lagrangian floats (D’Asaro, 2003) were deployed near the central mooring at (24°35'N, 38°W) in September 2012 and April 2013 (Figure 2b). Each float was equipped with two Sea-Bird SBE41 CTD sensors that were mounted on the top and the bottom of the hull, and an additional surface temperature-salinity (STS) probe at the top. The floats sampled the thermohaline structure of the upper ocean for five to six months each, typically collecting between eight and 14 profiles a day (both up- and downcasts). An accurate buoyancy control mechanism and a set of deployable drogue panels allowed the floats to reduce the profiling speed to 5–10 cm s<sup>-1</sup> near the surface. The slow profiling combined with the 1 Hz sampling rate of the STS allowed subdecimeter resolution of near-surface stratification. Between the profiles, Lagrangian floats were either parked just below the mixed layer at 60–150 m depth or drifted freely as fully Lagrangian particles following the mixed-layer turbulence and continuously sampling their environment. Lateral

advection of Lagrangian floats was more representative of the mean flow of the mixed layer and upper pycnocline, as opposed to the slower advection of APEX floats that spent considerable time at their typical parking depth of 1–2 km.

## INTERLEAVING AND THE ORIGINS OF SUBTROPICAL UNDERWATER

The properties and structure of STUW are largely set at the site of its last contact with the atmosphere in the core of the high surface salinity region. Even though the climatological subsurface maximum in vertical profiles of salinity associated with STUW does not extend north of ≈ 24°N in this region (Figure 1f), historical Argo observations show that smaller-scale high-salinity intrusions are common throughout the area (Figure 2a). Some of these intrusions may represent newly subducted portions of STUW.

Subduction is an intermittent process, occurring at the time of maximum density and thickness of the surface mixed layer, typically at the end of winter (Stommel, 1979; Williams, 2001). Patchiness of subduction can also be caused by local enhancement of vertical velocities associated with the submesoscale dynamics of upper-ocean fronts (Lévy et al., 2001; Mahadevan and Tandon, 2006; Thomas et al., 2008; Yoshikawa et al., 2012).

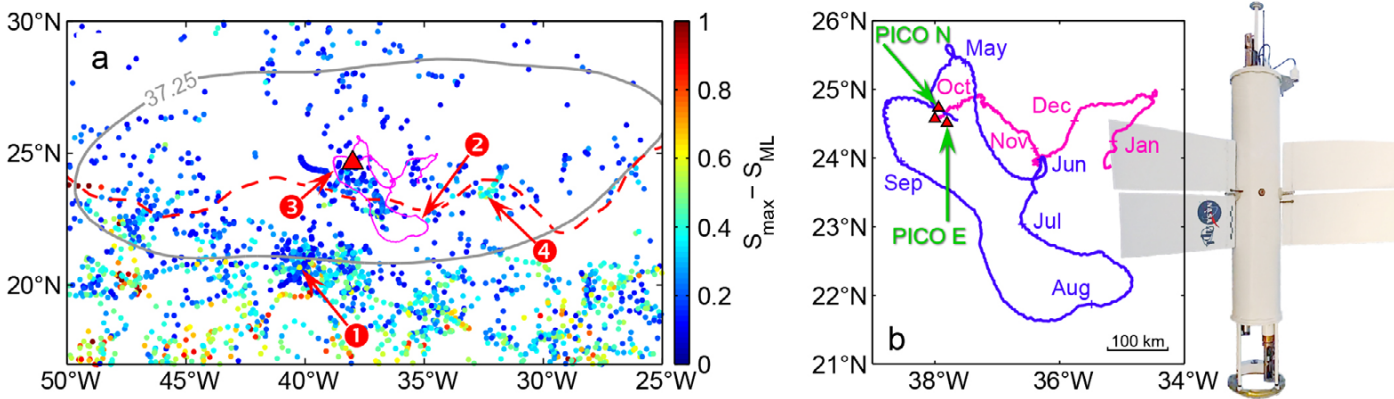


**FIGURE 2.** (a) Subsurface salinity maxima are commonly found throughout the region, even beyond the northernmost extent of the climatological subsurface salinity maximum (red dashed line). Locations of historic Argo float observations of subsurface salinity maxima are shown, color-coded by the difference between the maximum ( $S_{max}$ ) and mixed-layer ( $S_{ML}$ ) salinity. The climatological annual-mean 37.25 isohaline is shown in gray for cross-referencing with Figure 1. The red triangle marks the location of the SPURS-1 moorings. The numbered arrows point to the locations mentioned in the text. The magenta lines show the tracks of the Lagrangian floats. (b) Zoom-in on the Lagrangian float tracks, with labels showing the monthly progression. The SPURS-1 mooring array is marked with red triangles; green arrows point to the northern and eastern Platform and Instrumentation for Continuous Observations (PICO) moorings. A Lagrangian float photograph is at right.

Unlike the broad climatological vertical salinity profile maximum, individual intrusions commonly show a complex structure of interleaving layers (Figure 3). Such layering could potentially result from the patchiness and intermittency of subduction. Alternatively, it could be produced by secondary stirring and filamentation of the subducted lenses of STUW by the upper-ocean turbulent eddy field (Badin et al., 2011).

Insight into the variability of the vertical water mass layering can be gained from analysis of diapycnal spiciness curvature (DSC), a sensitive and robust indicator of interleaving activity. High absolute values of DSC indicate vertical interfaces between interleaving water masses (see Box 1 for details). Time series of root-mean-square (rms) DSC, compiled from three years of historic Argo float observations in the North Atlantic salinity maximum region, show a clear seasonal cycle of interleaving (Figure 4). In the density range of the STUW ( $\sigma_0 = 25.5 \pm 0.25 \text{ kg m}^{-3}$ ), maximum interleaving intensity occurs in April, roughly coinciding with the rapid restratification of deep wintertime mixed layers occurring in spring (Figure 1e). The seasonal cycle of interleaving extends to deeper layers ( $\sigma_0 = 26.5 \pm 0.25 \text{ kg m}^{-3}$ ), which do not outcrop in this area and therefore are not directly ventilated by local subduction. This supports the hypothesis that some subduction occurs through upper-pycnocline lateral stirring by mixed-layer submesoscale processes (Badin et al., 2011). Springtime enhancement of interleaving is consistent with the expected seasonality of submesoscale dynamics in the upper ocean, enhanced during the springtime restratification of deep wintertime mixed layers (Mahadevan et al., 2012; Mensa et al., 2013; Shcherbina et al., 2013).

Multiple interleaving features were observed by the moored Prawler profilers deployed at the northern and eastern PICO moorings (Figure 5). Starting in November, the diapycnal spiciness curvature (Figure 5b) increased, marking an

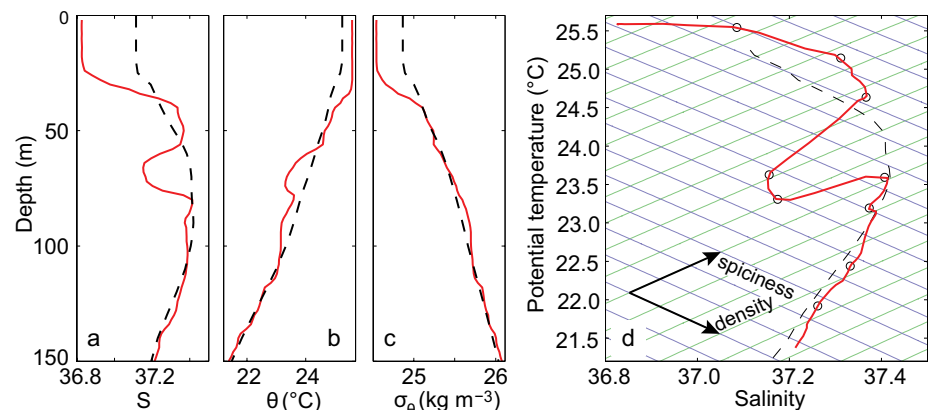


**FIGURE 3.** An example of vertical interleaving in STUW, as revealed by the vertical profiles of (a) salinity, (b) potential temperature, (c) potential density, and (d) the corresponding  $\theta$ -S diagram. An Argo float cast at  $20^{\circ}40'N$ ,  $40^{\circ}14'W$  (location 1 in Figure 2), on May 29, 2013, is shown in red, overlaid on the MIMOC monthly climatology profiles for the same location (dashed black line). Lines of constant potential density (green) and spiciness (blue) are shown in (d), with the arrows pointing in the direction of the increase of each parameter. Circles indicate the local extrema of diapycnal spiciness curvature that mark the interfaces of interleaving water masses.

### Box 1. Diapycnal Spiciness Curvature: An Interleaving Indicator

The concept of a “water mass” as a cluster of points in temperature-salinity ( $T$ - $S$ ) space goes back to Helland-Hansen (1916), who suggested that deviations from a “normal”  $T$ - $S$  profile mark intrusions of a disparate water mass (Worthington, 1981). Because seawater density depends on both temperature and salinity<sup>1</sup>, water masses of the same density can have different  $T$ - $S$  properties. To describe such isopycnal variations of temperature and salinity, a state variable of “spiciness” with the dimensions of density ( $\text{kg m}^{-3}$ ) is introduced (Figure 3d), reflecting how warm and salty the water of a given density is (Flament, 2002). Isopycnal interleaving and water mass intrusions can therefore be diagnosed as deviations of spiciness from some unperturbed background state of the ocean. Unfortunately, defining such a background state is often problematic.

Shcherbina et al. (2009) proposed an alternative intrusion indicator—diapycnal spiciness curvature (DSC), a second derivative of spiciness with respect to potential density along a profile. High absolute values of DSC indicate vertical interfaces between dissimilar water masses, characteristic of interleaving or local water mass modification (e.g., ventilation). In the absence of lateral advection, diapycnal mixing eventually destroys spiciness curvature, so DSC of an established water mass tends to be zero (Schmitt, 1981). DSC has a number of useful properties: it is dynamically justified, insensitive to background stratification, and not affected by vertical strain or displacement caused by internal waves (Shcherbina et al., 2009). It is also intuitive: high absolute values of DSC correspond to the “kinks” in the  $T$ - $S$  diagram (Figure 3d). The DSC-based method of interleaving analysis highlights small-scale instantaneous disturbances in the water mass structure; it is therefore complementary to the traditional anomaly method that focuses on the time-integral effects of water mass interleaving instead.

<sup>1</sup>Here, we neglect the effect of pressure on temperature and density (i.e., implying potential temperature and potential density, respectively).

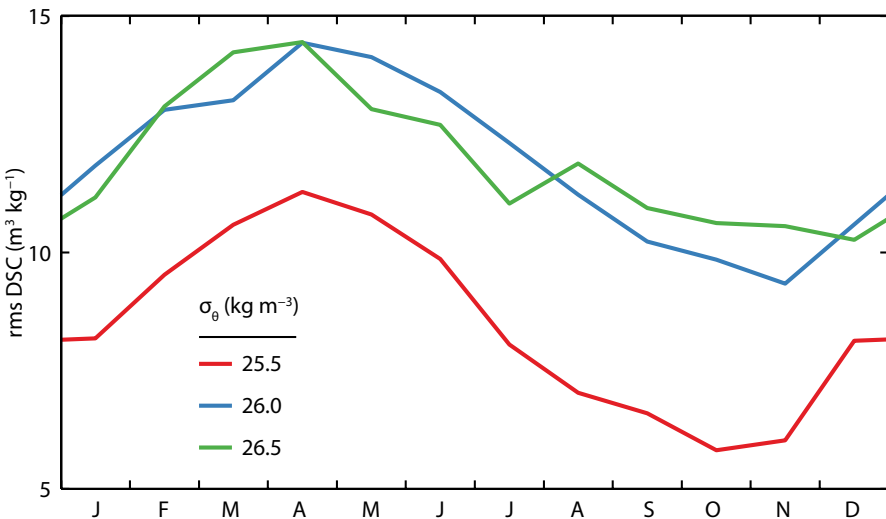


**FIGURE 4.** Maximum interleaving intensity in the North Atlantic salinity maximum region ( $15\text{--}30^\circ\text{N}$ ,  $25\text{--}55^\circ\text{W}$ ) occurs during the early spring (March to April). Root-mean-square diapycnal spiciness curvature values (rms DSC) for three potential density classes ( $\pm 0.25 \text{ kg m}^{-3}$ ) are shown. A total of 8,714 historic Argo float profiles between August 1, 2011, and August 1, 2014, were analyzed.

amplification of interleaving. This coincided with the seasonal deepening of the mixed layer to 75–100 m and enhancement of mesoscale activity in the pycnocline, as evidenced by highly variable isopycnal depths (Figure 5ab). A transient vertical salinity profile maximum in the range of STUW densities ( $\sigma_0 = 25.7 \text{ kg m}^{-3}$ ) was episodically observed at the mooring from December to January (Figure 5, inset). The vertical maximum was formed by the increase of salinity at 75–100 m depth by about 0.05, happening abruptly over the two-hour interval between the successive profiles. In at least two instances, the mid-depth salinity increases were accompanied by nearly simultaneous near-surface salinity decreases of about the same magnitude.

Opposing salinity changes at the top and bottom of the mixed layer suggest

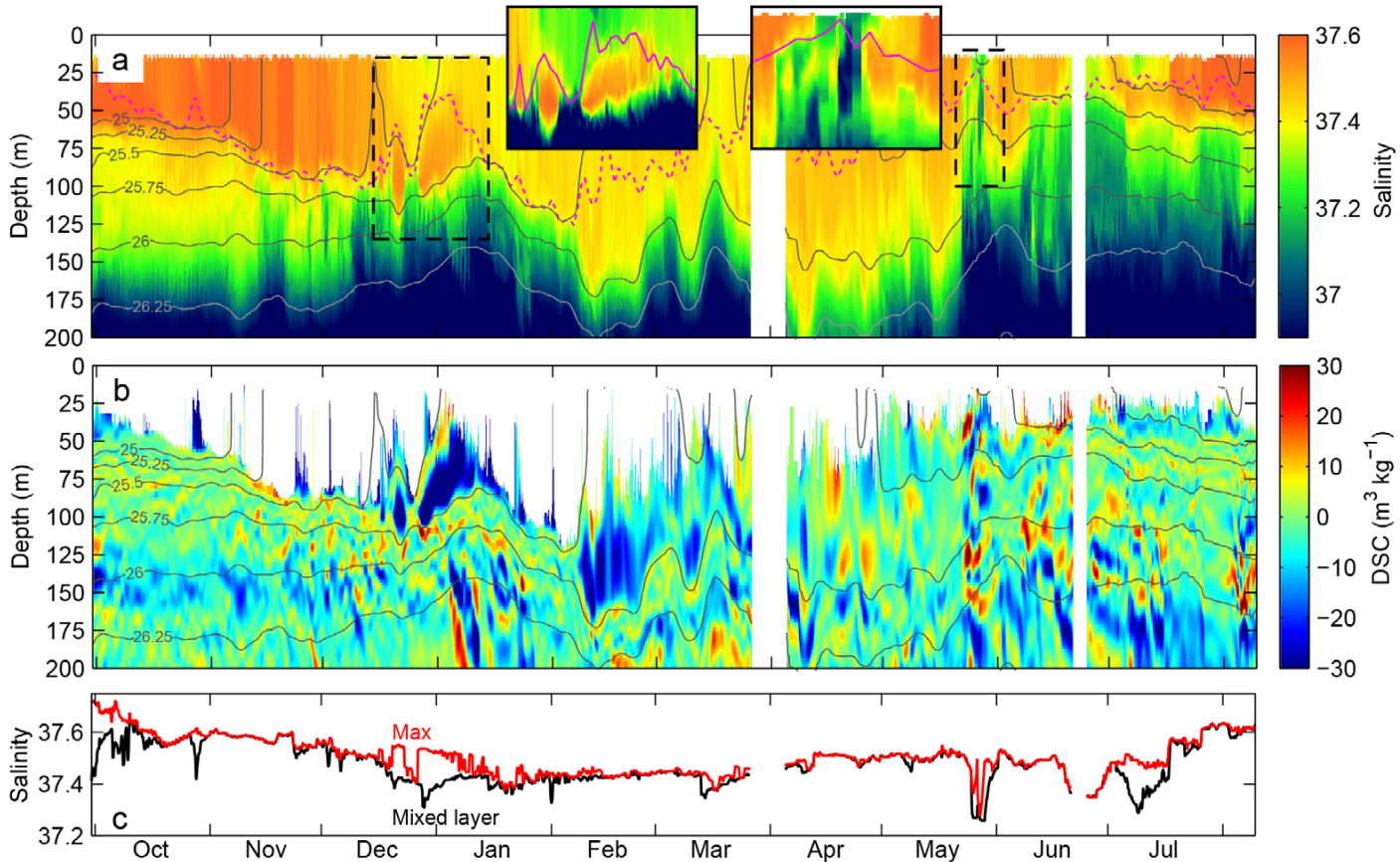


**FIGURE 5.** A moored profiler deployed at the surface salinity maximum core revealed multiple instances of vertical salinity interleaving features. Observations of (a) salinity and (b) diapycnal spiciness curvature are shown. The bottom panel (c) shows the evolution of the maximum (red) and mixed-layer (black) salinities. Potential density contours are overlaid on (a–b). Insets show examples of salinity interleaving (marked with dashed black boxes) with enhanced color contrast. The magenta line marks the mixed-layer depth. A composite of the northern (September to March) and eastern (April to August) Prawler records is shown.

that the interleaving structure was formed by “slumping” associated with baroclinic instabilities of a deep mixed-layer front (Boccaletti et al., 2007). In this scenario, sharp horizontal density gradients in the vertically homogeneous mixed layer release energy through the opposing lateral sliding of the denser water under the lighter water. As a result, the initially vertical isopycnals within the mixed layer become tilted, and the horizontal density gradients are converted to vertical stratification. Due to Earth’s rotation, the adjustment takes the form of submesoscale (1–10 km) eddies and filaments extending vertically across the original mixed-layer depth. Temperature and salinity fields are similarly affected by the slumping process, which produces opposing submesoscale thermohaline anomalies both at the original base of the mixed layer and near the surface.

Even though the Prawler mooring was located near the climatological surface salinity maximum, salinity gradients of  $2 \times 10^{-6} \text{ m}^{-1}$  (salinity change of 0.2 over 100 km distance) were occasionally present (Farrar et al., 2015, in this issue). Typical kilometer-scale gradients observed by SPURS Wave Gliders had long-term rms values of  $5.5 \times 10^{-6} \text{ m}^{-1}$  (Benjamin Hedges, Woods Hole Oceanographic Institution, pers.

comm., 2014). The 0.05 salinity changes observed in the intrusion thus correspond to about 10 km of lateral displacement of a typical gradient, an amount that could easily be accomplished by submesoscale eddies. With deepening of mixed layers in winter, these small-scale gradients become increasingly susceptible to baroclinic mixed-layer instabilities, which slump the fronts and subduct the denser saltier water to create the observed subsurface intrusions near the base of the mixed layer (Thomas et al., 2008). Such seasonal mixed-layer restratification can be seen as the first step in the subduction and formation of STUW.

Similar, but more prominent, high-salinity intrusions in the upper pycnocline were also observed by the Lagrangian floats the following summer (July to August) further south, at  $22^{\circ}\text{--}24^{\circ}\text{N}$  (Figure 6). Unlike the wintertime intrusions seen at the Prawler moorings, the summertime features were deeper than the typical mixed-layer depth at that time, suggesting that they were formed by subduction at another location or time, most likely during the previous winter.

Episodic freshening of the upper 20–50 m of the water column was also observed by the Prawler moorings and Lagrangian floats. The smaller of these events were due to local rainstorms, as

discussed in detail by Riser et al. (2015, in this issue); the larger were the results of advection of fresh mesoscale lenses, similar to those observed by Busecke et al. (2014) in the same area from March to April 2013. Some of these surface freshening events were seemingly associated with the high-salinity intrusions discussed earlier (e.g., July to August events observed by the Lagrangian float; Figure 6), while others were not (e.g., early July event observed by the Prawler moorings, Figure 5, and the ones discussed by Busecke et al., 2014). It is presently not clear whether this occasional association of upper-thermocline high-salinity features and shallow fresh lenses is purely coincidental or whether it is a remnant signature of the original two-layer slumping instability.

Lagrangian and APEX float records showed multiple instances of rapid changes and fragmentation of vertical interleaving structure. Figure 7 shows an example of one such change, as observed by a SPURS APEX float in September 2013 approximately 600 km southeast of the SPURS-1 site. Data from the float show a breakup of a single broad salinity maximum into a series of thinner interleaving layers with alternating vertical salinity gradients. The layers were predominantly isopycnal and had a vertical

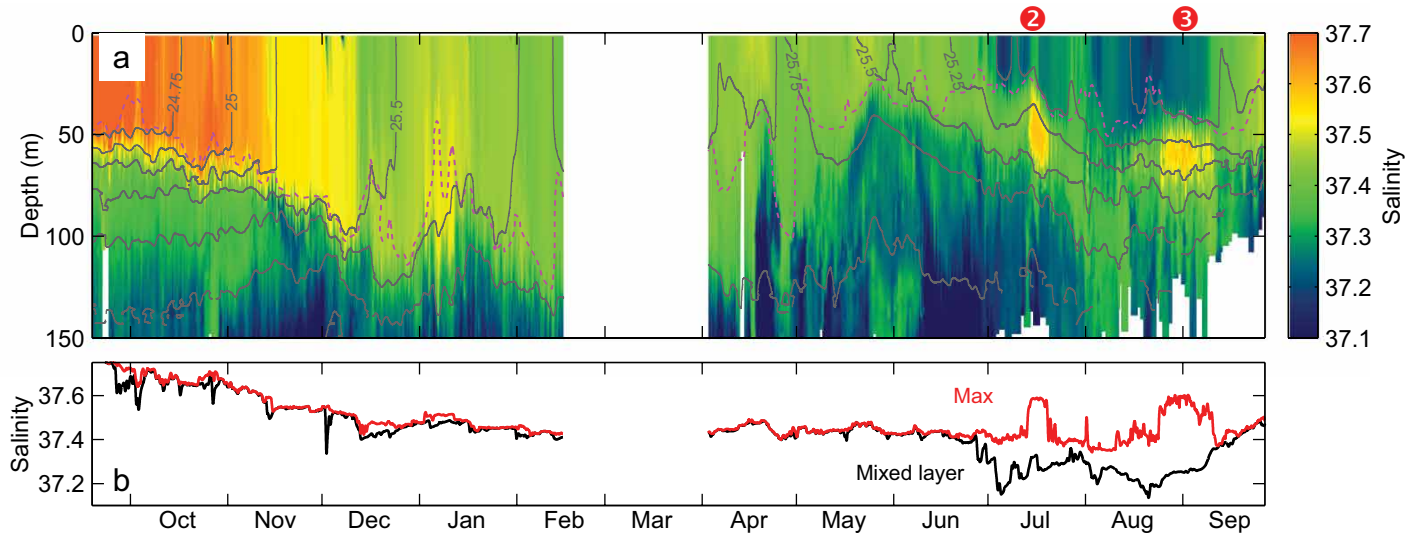


**FIGURE 6.** Lagrangian float observations of salinity, showing an alternative (Lagrangian) view of the evolution of upper-ocean interleaving. The magenta dashed line marks the mixed-layer depth. The lower panel (b) shows the evolution of the maximum (red) and mixed-layer (black) salinities. Numbers (2) and (3) mark the timing of two prominent high-salinity intrusions, corresponding to along-track location markers (2) and (3) in Figure 2a.

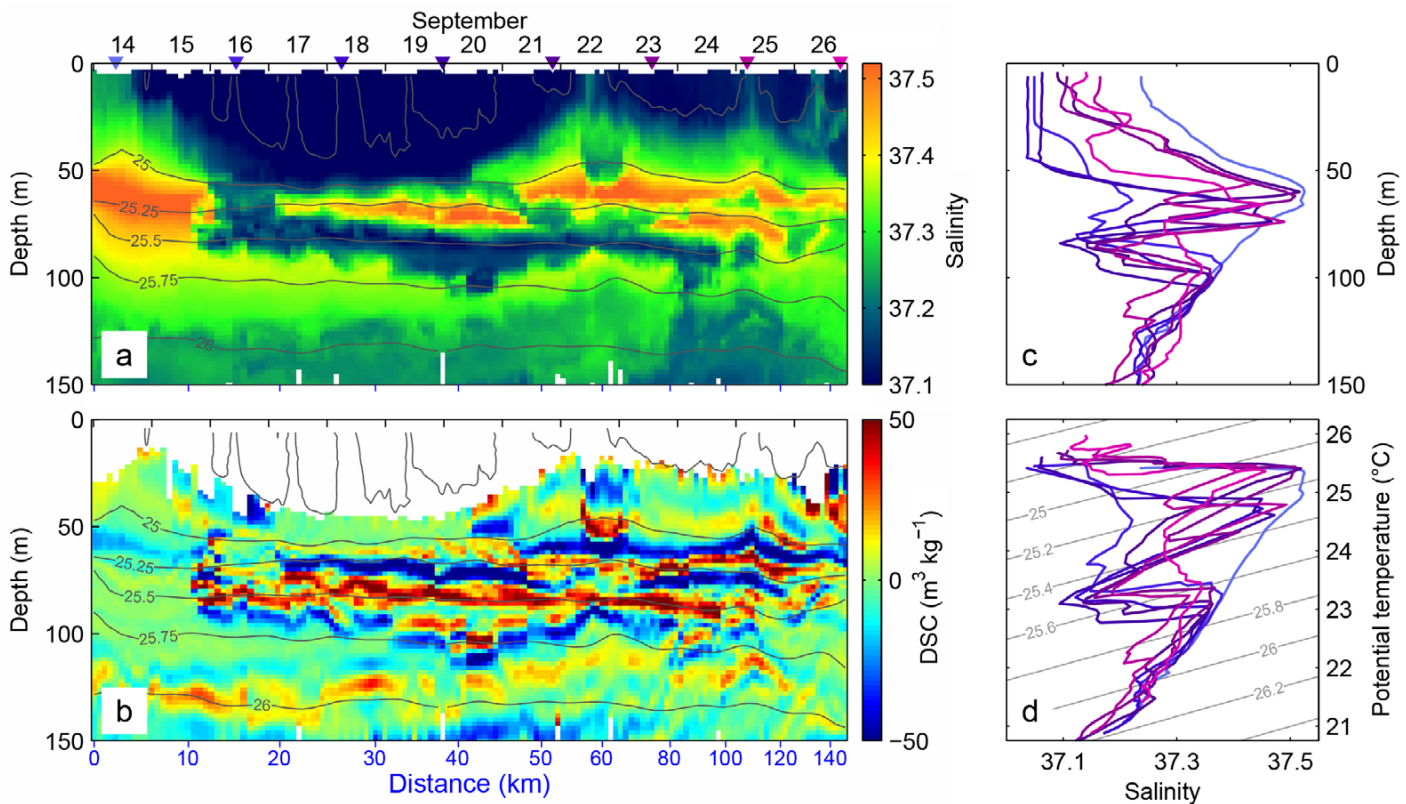


**FIGURE 7.** An example of a salinity maximum breaking into a series of dynamic interleaving features over the course of several days. Time-depth sections of (a) salinity and (b) diapycnal spiciness curvature, with potential density contours overlaid. Distance along the float drift trajectory is shown along the bottom. Individual salinity profiles vs. (c) depth and (d) potential temperature are shown on the right, color-coded by time; timing is indicated by the coordinating colored triangles in (a). Distortions due to internal waves have been eliminated in (a–c) by removing subinertial isopycnal displacements (i.e., adopting a local semi-Lagrangian vertical coordinate). Observations were made with a fast-cycling APEX float at 23°21'N, 32°23'W, approximately 600 km ESE of the SPURS site (location 4 in Figure 2).

scale of about 15 m (peak-to-trough). The radical changes in stratification observed in the neighboring profiles separated by less than a kilometer and taken only several hours apart indicate that these features are submesoscale. Strong interleaving at these small scales suggests that additional stirring processes act to break up the STUW intrusions, transforming the initially variable water mass profile formed in winter (e.g., Figure 3) into the smoother, broader profile found further away from the formation site.

## CONCLUSIONS

STUW is an intermediate water mass originating in the surface salinity maximum of the central Atlantic. Its salinity acts as a tracer of the subduction processes that move surface water into the interior and drive the subtropical cell of the oceanic overturn. STUW subduction is therefore expected to play a vital

role in decadal climate variability across the tropics. At the same time, this shallow and dynamic water mass may also be a sensitive indicator for the emerging changes in global climate.

The SPURS-1 observations portray STUW subduction as a highly variable, inhomogeneous, and dynamic process that is strongest in late winter–early spring and unevenly distributed in space, perhaps concentrated at kilometer-scale surface frontal regions. As such, accurate representation of the STUW origins in global climate models is challenging and requires detailed understanding and parameterization of the underlying multi-scale interactions. Though the NASA SPURS project has been focused to date on the North Atlantic, similar subduction processes drive the shallow thermohaline overturns and formation of intermediate water masses across subtropical regions of the entire ocean. Further synthesis

of the SPURS-1 results, combined with global observations of surface salinity by the Aquarius/SAC-D (Lagerloef, 2012) and Soil Moisture and Ocean Salinity (SMOS) (Font et al., 2010) satellite missions, will provide insight into processes controlling mixing and redistribution of salt and freshwater in the ocean and improve our understanding of the interconnections of ocean circulation, the global water cycle, and climate. ☐

**ACKNOWLEDGEMENTS.** We are grateful to the research and technical members of the SPURS team who made these observations possible. We thank NASA, and particularly Eric Lindstrom, for support of the SPURS program. Editorial assistance by J. Lundquist is gratefully acknowledged. This work was supported by NASA grants NNX11AE81G (AS, EDA) and NNX11AF79G (SR). The Prawler moorings were funded by PMEL, and this is PMEL Contribution #4251. Historical Argo float data were collected and made freely available by the International Argo Project and the national programs that contribute to it (<http://www.argo.net>). The Argo Program is part of the Global Ocean Observing System.

## REFERENCES

- Badin, G., A. Tandon, and A. Mahadevan. 2011. Lateral mixing in the pycnocline by baroclinic mixed layer eddies. *Journal of Physical Oceanography* 41:2,080–2,101, <http://dx.doi.org/10.1175/JPO-D-11-051>.
- Boccaletti, G., R. Ferrari, and B. Fox-Kemper. 2007. Mixed layer instabilities and restratification. *Journal of Physical Oceanography* 37(9):2,228–2,250, <http://dx.doi.org/10.1175/JPO3101.1>.
- Busecke, J., A.L. Gordon, Z. Li, F.M. Bingham, and J. Font. 2014. Subtropical surface layer salinity budget and the role of mesoscale turbulence. *Journal of Geophysical Research: Oceans* 119(7):4,124–4,140, <http://dx.doi.org/10.1002/2013JC009715>.
- Curry, R., B. Dickson, and I. Yashayaev. 2003. A change in the freshwater balance of the Atlantic Ocean over the past four decades. *Nature* 426(6968):826–829, <http://dx.doi.org/10.1038/nature02206>.
- D'Asaro, E.A. 2003. Performance of autonomous Lagrangian floats. *Journal of Atmospheric and Oceanic Technology* 20(6):896–911, [http://dx.doi.org/10.1175/1520-0426\(2003\)020<0896:POALF>2.0.CO;2](http://dx.doi.org/10.1175/1520-0426(2003)020<0896:POALF>2.0.CO;2).
- Farrar, J.T., L. Rainville, A.J. Plueddemann, W.S. Kessler, C. Lee, B.A. Hodges, R.W. Schmitt, J.B. Edson, S.C. Riser, C.C. Eriksen, and D.M. Fratantoni. 2015. Salinity and temperature balances at the SPURS central mooring during fall and winter. *Oceanography* 28(1):56–65, <http://dx.doi.org/10.5670/oceanog.2015.06>.
- Flament, P. 2002. A state variable for characterizing water masses and their diffusive stability: Spiciness. *Progress in Oceanography* 54(1–4):493–501, [http://dx.doi.org/10.1016/S0079-6611\(02\)00065-4](http://dx.doi.org/10.1016/S0079-6611(02)00065-4).
- Font, J., A. Camps, A. Borges, M. Martin-Neira, J. Boutin, N. Reul, Y.H. Kerr, A. Hahne, and S. Mecklenburg. 2010. SMOS: The challenging sea surface salinity measurement from space. *Proceedings of the IEEE* 98(5):649–665, <http://dx.doi.org/10.1109/JPROC.2009.2033096>.
- Gordon, A.L., C.F. Giulivi, J. Busecke, and F.M. Bingham. 2015. Differences among subtropical surface salinity patterns. *Oceanography* 28(1):32–39, <http://dx.doi.org/10.5670/oceanog.2015.02>.
- Helland-Hansen, B. 1916. Nogen hydrografiske metoder. *Skandinaviske Naturforskermote* 16:357–359.
- Lagerloef, G. 2012. Satellite mission monitors ocean surface salinity. *Eos, Transactions American Geophysical Union* 93:233–234, <http://dx.doi.org/10.1029/2012EO250001>.
- Lévy, M., P. Klein, and A.-M. Treguier. 2001. Impact of sub-mesoscale physics on production and subduction of phytoplankton in an oligotrophic regime. *Journal of Marine Research* 59:535–565, <http://dx.doi.org/10.1357/002224001762842181>.
- Lindstrom, E., F. Bryan, and R. Schmitt. 2015. SPURS: Salinity Processes in the Upper-ocean Regional Study—The North Atlantic Experiment. *Oceanography* 28(1):14–19, <http://dx.doi.org/10.5670/oceanog.2015.01>.
- Mahadevan, A., E. D'Asaro, C. Lee, and M.J. Perry. 2012. Eddy-driven stratification initiates North Atlantic spring phytoplankton blooms. *Science* 337:54–58, <http://dx.doi.org/10.1126/science.1218740>.
- Mahadevan, A., and A. Tandon. 2006. An analysis of mechanisms for submesoscale vertical motion at ocean fronts. *Ocean Modelling* 14:241–256, <http://dx.doi.org/10.1016/j.ocemod.2006.05.006>.
- McCreary, J.P., and P. Lu. 1994. Interaction between the subtropical and equatorial ocean circulations: The subtropical cell. *Journal of Physical Oceanography* 24:466–497.
- Mensa, J., Z. Garraffo, A. Griffa, T. Özgökmen, A. Haza, and M. Veneziani. 2013. Seasonality of the submesoscale dynamics in the Gulf Stream region. *Ocean Dynamics* 63:923–941, <http://dx.doi.org/10.1007/s10236-013-0633-1>.
- Nonaka, M., S.-P. Xie, and J.P. McCreary. 2002. Decadal variations in the subtropical cells and equatorial pacific SST. *Geophysical Research Letters* 29(7), <http://dx.doi.org/10.1029/2001GL013717>.
- O'Connor, B.M., R.A. Fine, and D.B. Olson. 2005. A global comparison of subtropical underwater formation rates. *Deep Sea Research Part I* 52:1,569–1,590, <http://dx.doi.org/10.1016/j.dsri.2005.01.011>.
- Qu, T., S. Gao, and I. Fukumori. 2013. Formation of salinity maximum water and its contribution to the overturning circulation in the North Atlantic as revealed by a global general circulation model. *Journal of Geophysical Research* 118:1,982–1,994, <http://dx.doi.org/10.1002/jgrc.20152>.
- Riser, S.C., J. Anderson, A. Shcherbina, and E. D'Asaro. 2015. Variability in near-surface salinity from hours to decades in the eastern North Atlantic: The SPURS region. *Oceanography* 28(1):66–77, <http://dx.doi.org/10.5670/oceanog.2015.11>.
- Schmidtko, S., G.C. Johnson, and J.M. Lyman. 2013. MIMOC: A global monthly isopycnal upper-ocean climatology with mixed layers. *Journal of Geophysical Research* 118:1,658–1,672, <http://dx.doi.org/10.1002/jgrc.20122>.
- Schmitt, R.W. 1981. Form of the temperature–salinity relationship in the central water: Evidence for double-diffusive mixing. *Journal of Physical Oceanography* 11:1,015–1,026, [http://dx.doi.org/10.1175/1520-0485\(1981\)011<1015:FOTTSR>2.0.CO;2](http://dx.doi.org/10.1175/1520-0485(1981)011<1015:FOTTSR>2.0.CO;2).
- Schmitt, R.W., and A. Blair. 2015. A river of salt. *Oceanography* 28(1):40–45, <http://dx.doi.org/10.5670/oceanog.2015.04>.
- Shcherbina, A.Y., E.A. D'Asaro, C.M. Lee, J.M. Klymak, M.J. Molemaker, and J.C. McWilliams. 2013. Statistics of vertical vorticity, divergence, and strain in a developed submesoscale turbulence field. *Geophysical Research Letters* 40:4,706–4,711, <http://dx.doi.org/10.1002/grl.50919>.
- Shcherbina, A.Y., M.C. Gregg, M.H. Alford, and R.R. Harcourt. 2009. Characterizing thermo-haline intrusions in the North Pacific subtropical frontal zone. *Journal of Physical Oceanography* 39:2,735–2,756, <http://dx.doi.org/10.1175/2009JPO4190.1>.
- Stommel, H. 1979. Determination of water mass properties of water pumped down from the Ekman layer to the geostrophic flow below. *Proceedings of the National Academy of Sciences of the United States of America* 76:3,051–3,055, <http://www.pnas.org/content/76/7/3051.full.pdf>.
- Talley, L.D. 2002. Salinity patterns in the ocean. Pp. 629–640 in *Encyclopedia of Global Environmental Change, Volume, The Earth System: Physical and Chemical Dimensions of Global Environmental Change*. M.C. MacCracken and J.S. Perry, eds, John Wiley & Sons, Chichester.
- Thomas, L.N., A. Tandon, and A. Mahadevan. 2008. Submesoscale processes and dynamics. Pp. 17–38 in *Ocean Modeling in an Eddying Regime*. M.W. Hecht and H. Hasumi, eds, American Geophysical Union, Washington, DC.
- Williams, R.G. 2001. Ocean subduction. Pp. 1,982–1,992 in *Encyclopedia of Ocean Sciences*. J.H. Steele, K.K. Turekian, and S.A. Thorpe, eds, Academic Press, Oxford.
- Worthington, L.V. 1981. The water masses of the world ocean: Some results of a fine scale census. Pp. 42–69 in *Evolution of Physical Oceanography*. B.A. Warren and C. Wunsch, eds, MIT Press, Cambridge, MA.
- Yoshikawa, Y., C.M. Lee, and L.N. Thomas. 2012. The subpolar front of the Japan/East Sea. Part III: Competing roles of frontal dynamics and atmospheric forcing in driving geostrophic vertical circulation and subduction. *Journal of Physical Oceanography* 42:991–1,011, <http://dx.doi.org/10.1175/JPO-D-11-0154.1>.

**AUTHORS.** Andrey Y. Shcherbina ([shcher@uw.edu](mailto:shcher@uw.edu)) is Senior Oceanographer, Applied Physics Laboratory, University of Washington, Seattle, WA, USA. Eric A. D'Asaro is Senior Principal Oceanographer, Applied Physics Laboratory, and Professor of Oceanography, University of Washington, Seattle, WA, USA. Stephen C. Riser is Professor of Oceanography, University of Washington, Seattle, WA, USA. William S. Kessler is Oceanographer, Pacific Marine Environmental Laboratory/National Oceanic and Atmospheric Administration, and Affiliate Professor of Oceanography, University of Washington, Seattle, WA, USA.

## ARTICLE CITATION

Shcherbina, A.Y., E.A. D'Asaro, S.C. Riser, and W.S. Kessler. 2015. Variability and interleaving of upper-ocean water masses surrounding the North Atlantic salinity maximum. *Oceanography* 28(1):106–113, <http://dx.doi.org/10.5670/oceanog.2015.12>.